Digest Journal of Nanomaterials and Biostructures

Dig. J. Nanomater. Bios. **2026**; 21(3): 57889
https://doi.org/10.31083/DJNB57889

Original Research

Adsorption Selectivity of Thiophene and Benzene on Metal Ion–Modified Nanoporous M-HY Zeolites: A Theoretical Mechanistic Study

Yu Hua Guo[1,*], Min Hong Xu[1], Guo Xiang Pan[1,2], Kun Yan Wang[1], Qing Zhang[1]

[1]Zhejiang Key Laboratory for Industrial Solid Waste Thermal Hydrolysis Technology, Intelligent Equipment and Huzhou Key Laboratory of Environmental Functional Materials and Pollution Control, Department of Materials Engineering, Huzhou Normal University, 313000 Huzhou, Zhejiang, China

[2]Zhejiang Huayuan Pigment Co., Ltd., 313220 Deqing, Zhejiang, China

*Correspondence: guoyuhua@zjhu.edu.cn (Yu Hua Guo)

Academic Editor: Maria Harja

Submitted: 12 January 2026 Revised: 12 April 2026 Accepted: 29 April 2026 Published: 11 September 2026

Abstract

Background: The desulfurization of fuel oil is of great importance for environmental protection. A core challenge of adsorptive desulfurization is the difficulty in achieving the highly selective adsorption of trace organic sulfur compounds in real fuel systems characterized by the copresence of diverse aromatics and other competitors. **Method:** The mechanism of adsorption selectivity between thiophene and benzene on metal ions (M = Al^{3+}, Ti^{3+}, Mn^{3+}, Co^{3+}, Cu^{2+}, and Zn^{2+})-modified M-Hydrogen Y zeolite (M-HY zeolites) was systematically elucidated using our own N-layered integrated molecular orbital and molecular mechanics (ONIOM) method. **Results:** All metal ions could be incorporated into the zeolite framework without markedly disrupting the pore structure. Brønsted acid strength followed the order of Ti-HY > Mn-HY > Al-HY > Co-HY > Zn-HY ≈ Cu-HY, and both thiophene and benzene were adsorbed by forming π-complexes with the acid sites. The energies of thiophene and benzene adsorption on Al-, Ti-, Mn-, and Zn-HY zeolites were comparable (70–79 kJ/mol), indicating poor selectivity. In contrast, the energies of benzene adsorption on Co-HY and Cu-HY zeolites were 39.66 and 36.74 kJ/mol higher than those of thiophene, respectively, implying the preferential adsorption of benzene. **Conclusions:** Adsorption performance was governed by acid strength, framework structure, and the intrinsic properties of the adsorbate molecules; selective adsorption could not be achieved by simply increasing the number of acid sites. This study provides a theoretical basis for the design of highly selective desulfurization adsorbents and highlights the need to move beyond the conventional π-complexation mechanism toward enhancing specific S-M interactions.

Keywords: thiophene; benzene; zeolite; adsorption mechanism; ONIOM

1. Introduction

Sulfur compounds in fuel oil are a major source of air pollution. As fuel oil consumption continues to rise globally, the environmental impact of its sulfur content has become increasingly severe. In response, countries have imposed stricter regulations on sulfur levels in fuel oil products. Consequently, the development of efficient desulfurization technologies for clean fuel production has emerged as a research hotspot in recent years [1,2,3]. At present, there are two main technologies for producing clean fuel oil: hydrodesulfurization and non-hydrodesulfurization. Hydrodesulfurization is the most commonly used method in oil refineries and is highly effective for removing mercaptans and thioether compounds. However, deep removal technology for thiophene and its derivatives has yet to achieve a major breakthrough, and existing research results cannot meet the requirements for industrial application. Non-hydrodesulfurization methods mainly include biological desulfurization, adsorptive desulfurization, extraction desulfurization, and oxidative desulfurization. Among these, adsorptive desulfurization is a new desulfurization technology developed in recent years [4,5,6]. This method can produce low-sulfur or even sulfur-free gasoline under mild conditions. The adsorbent, after regeneration, can be used cyclically, requiring less investment and offering low operating costs. Therefore, it is considered the most promising method for achieving deep desulfurization targets. The composition of fuel oil is inherently complex. In addition to containing thiophene and its alkylated derivatives, fuel oil also contains a certain amount of benzene and its derivatives, as well as numerous straight-chain and branched-chain alkanes. This requires that the deep desulfurization adsorbent must have excellent selectivity for thiophene and its derivatives, minimizing the adsorption of other components to prevent a decrease in adsorption capacity and a reduction in selectivity. Therefore, the core of adsorptive desulfurization technology lies in developing adsorbents with high selectivity.

Currently, the most widely studied adsorbents mainly include activated carbon, metal-organic frameworks, zeolites, etc., each offering distinct advantages in structural characteristics and desulfurization performance [7,8,9].

Activated carbon possesses a high specific surface area and well-developed pore structure, and its adsorption performance can be enhanced through surface modification. However, its selectivity toward sulfur compounds is relatively weak, making it susceptible to competitive adsorption from aromatic hydrocarbons, which limits its desulfurization efficiency in actual complex fuel systems [7,10]. Metal-organic frameworks feature extremely high specific surface areas and tunable pore structures, enabling excellent adsorption capacity through unsaturated metal sites. Nevertheless, their poor hydrothermal stability leads to framework collapse, and challenges such as high synthesis costs, insufficient mechanical strength, and difficult regeneration pose significant barriers to industrial application [8,11]. Zeolites possess well-defined microporous structures, good thermal stability, and ion-exchange capability. After modification with metal ions, they achieve efficient and selective adsorption of thiophenic sulfur compounds [4,12]. Although their microporous structure imposes certain limitations on the diffusion of bulky sulfur compounds and metal components may be lost during regeneration, their overall performance, stability, and cost advantages still make them the most promising adsorbent materials for industrial adsorptive desulfurization applications [13,14]. Researchers have systematically investigated the adsorption desulfurization performance of various zeolite materials, including X-type, Y-type, β-type, MCM-41, and Zeolite Socony Mobil (ZSM) series [15,16,17,18,19]. Unlike zeolites with ten-membered ring pore structures (pore size ca. 0.55 nm), such as ZSM-5, Y-type nanoporous zeolite possesses a three-dimensional supercage structure (diameter ca. 1.3 nm) and twelve-membered ring windows (diameter ca. 0.74 nm), which provide favorable diffusion pathways and accessible adsorption sites for thiophene molecules (kinetic diameter ca. 0.53 nm), while also exhibiting significant shape selectivity [20,21]. Furthermore, HY zeolite can be modified via ion exchange to introduce metal cations (e.g., Ce^{3+}, Cu^{+}), enabling the construction of synergistic active centers combining Brønsted acid sites and metal species within the supercages, thereby substantially enhancing its adsorption capacity for thiophene sulfides [22]. Meanwhile, regulating the location of active sites within the supercages can effectively promote the selective adsorption of thiophene while suppressing competitive interference from aromatic hydrocarbons [23]. Based on these advantages, metal-ion-exchanged Y-type zeolite is considered a promising adsorbent for adsorption desulfurization (ADS) [24,25]. However, this material still faces challenges in practical applications, including insufficient selectivity, low sulfur capacity, poor regeneration performance, and inadequate stability. One of the critical factors restricting its further development is the lack of consensus regarding the mechanism of selective adsorption desulfurization [26,27,28,29]. Elucidating the adsorption mechanism in depth would not only provide a theoretical basis for the design and optimization of efficient adsorbents, but also serve as an essential foundation for advancing its practical application.

At present, two adsorptive desulfurization mechanisms have been proposed: π-complexation [30,31] and S-M metal complexation [32,33]. In addition, surface acidity of molecular sieves has been identified as a key factor influencing desulfurization efficiency, with increased acidity enhancing sulfur adsorption capacity [18,34]. However, experimental methods alone fail to reveal the location of adsorbates within molecular sieve cages or the interaction characteristics between the sieve and adsorbate molecules—information that is essential for the rational design of novel adsorptive separation materials. As a result, Quantum chemical methods are increasingly being used to complement experimental studies, providing deep insights into the nature of adsorption sites, binding energies, and host–guest interactions at the atomic scale [21,35,36]. For example, Wang et al. [35] employed density functional theory (DFT) to reveal the key roles of different exchanged metal cations (Cu^{+}, Ni^{2+}, Ce^{3+}) in modifying Y-type zeolites for thiophene compound adsorption, with Cu(I)Y exhibiting the highest adsorption capacity. Similarly, Gao et al. [36] through DFT calculations, found that charge transfer between the π electrons of thiophene rings and both rare-earth atoms and the zeolite framework plays a crucial role during the adsorption of thiophene compounds on rare-earth-ion-exchanged Y-type zeolites. Likewise, Sokol et al. [21], based on DFT studies, demonstrated that copper- and cerium-co-exchanged Y-type zeolites (CuCeY) show excellent adsorptive desulfurization performance, attributed to the synergistic effect between copper and cerium cations via electron sharing. These atomic-level understandings provide important guidance for designing high-performance adsorbents with tunable selectivity, high capacity, and good regenerability.

As a multilayer quantum mechanics/molecular mechanics (QM/MM) computational strategy, the our own N-layered integrated molecular orbital and molecular mechanics (ONIOM) method ensures high accuracy for large molecular systems while significantly reducing computational costs. This method has been successfully applied to investigate the adsorption behavior of unsaturated hydrocarbons on zeolites, enabling efficient synergistic calculations of the interactions between adsorption active centers and the framework environment [21,37,38,39]. It is worth noting, however, that most current simulation studies on adsorptive desulfurization employ zeolite cluster models in which metal ions are stabilized within the pores or near the active sites of Y-type zeolites. Although metal ions can also be introduced into the zeolite framework via in-situ synthesis methods [40,41], theoretical studies on the adsorption desulfurization mechanism of such framework-substituted zeolites remain scarce. To address this gap, this study systematically investigates M-Hydrogen Y zeolite (M-HY zeolites, M = Al^{3+}, Ti^{3+}, Mn^{3+}, Co^{3+}, Cu^{2+},

and Zn^{2+}) with metal ions incorporated directly into the framework, providing atomic-scale insights into the adsorption selectivity of thiophene and benzene under a unified ONIOM(B3LYP/UFF) framework. Accordingly, the adsorption selectivity mechanism between thiophene and benzene is elucidated, offering a theoretical basis for the development of novel selective adsorptive desulfurization materials.

2. Materials and Methods

To investigate the adsorption behavior of thiophene and benzene on zeolites modified with various metal ions, a 144T cluster model was extracted from the twelve-membered ring main channel of HY zeolite to simulate the structure of Y-type zeolite, with unit cell parameters of a = b = c = 25.028 Å [42] (see Fig. 1). The 144T cluster model is composed of 144 SiO_4 tetrahedra and includes a complete supercage structure. This supercage acts as a nanoscale adsorption cavity that can fully encapsulate the adsorbate molecules, thus fully capturing the influence of the framework environment on the adsorption process. Moreover, previous studies have demonstrated that supercage sites (especially site II) are most readily accessible to thiophene and benzene molecules, and the Brønsted acid sites involved in π-complex formation are also predominantly located within the supercage [20,21].

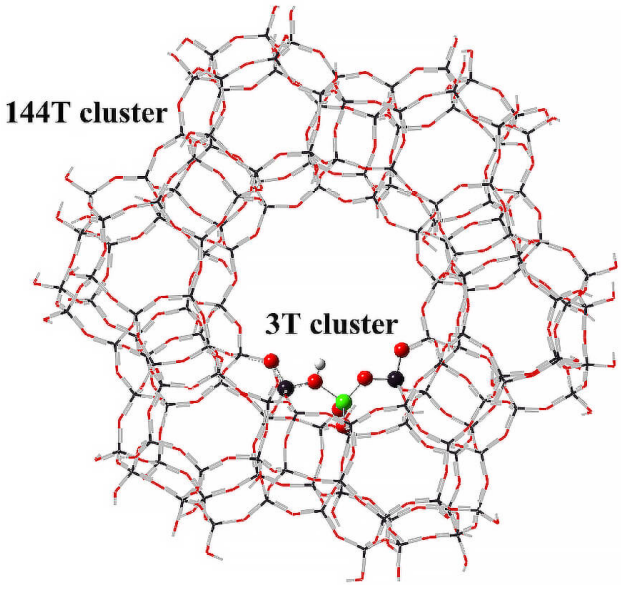

Fig. 1. Structure of the cluster model of the HY zeolite. HY zeolite, Hydrogen Y zeolite.

In this study, calculations were performed using the ONIOM method, and the model was divided into two layers. The inner active region was represented by a 3T cluster model [=OSiO(H)M(O)$_2$OSiO=] (M = Al^{3+}, Ti^{3+}, Mn^{3+}, Co^{3+}, Cu^{2+}, and Zn^{2+}) to characterize the acid sites of the zeolite. Calculations involving the 3T cluster model and adsorbate molecules were carried out using the DFT method at the B3LYP/6-31G(d,p) level to accurately describe the atoms involved in the interactions. The outer framework of the zeolite was treated with the universal force field (UFF) [43], which adequately describes the van der Waals interactions between adsorbate molecules and the zeolite [38,44]. Relevant studies have indicated that the adsorption energies of organic molecules in zeolites calculated using the ONIOM method combining B3LYP and UFF are in good agreement with experimental values [44,45,46].

It should be noted that thiophene and benzene were investigated separately through single-molecule adsorption calculations, rather than co-adsorption simulations, to determine their individual adsorption energies and geometric parameters on each M-HY zeolite. During geometry optimization, the 3T cluster model and the adsorbate molecule were fully optimized, while the remaining parts were fixed at their crystallographic coordinates. Vibrational frequencies were obtained at the same level of theory and scaled by a correction factor of 0.9614 [47]. All calculations were performed using the Gaussian 03 software package (Gaussian, Inc., Pittsburgh, PA, USA) [48].

3. Results

3.1 Metal Ions Modified M-HY Zeolite

The activity of zeolites is often related to the strength of their acid sites, which depends on the chemical composition and framework topology [49]. The acid sites in zeolites result from the isomorphous substitution of Si^{4+} cations by Al^{3+} cations, leading to the formation of bridged hydroxyl groups (Si-O(H)-Al), which act as strong Brønsted acid sites. Experimental studies have shown that other metal ions can also isomorphously substitute Si atoms in the framework and enter the zeolite framework [40,41,50]. However, detailed information regarding the coordination environment of metal cations cannot be obtained experimentally. The coordination structure and electronic properties of metal ions are particularly important for investigating the adsorption behavior and catalytic potential of these materials. Therefore, this study theoretically explores the possibility of metal ions entering the zeolite framework and their influence on the acidity of zeolites. The modified metal ions (M = Al^{3+}, Ti^{3+}, Mn^{3+}, Co^{3+}, Cu^{2+}, and Zn^{2+}) were positioned within the Y-type zeolite framework, and their configurations were optimized. The optimized structures of the M-HY zeolites are shown in Fig. 2, and the corresponding geometric parameters are summarized in Table 1. It can be observed that the geometric structure of the active site (3T cluster model) undergoes slight changes due to the doping of different metal ions. The O1-H1 bond distance (0.967–0.976 Å) exhibits very little variation, while the Si1-O1 and Si2-O2 bond distances (1.649–1.684 Å and 1.644–1.678 Å, respectively) also show only minor changes. The M1-O1 bond distances range from 1.908 to 2.083 Å, and the M1-O2 bond distances fall be-

tween 1.726 and 1.853 Å. The bond angles of Si1-O1-M1, M1-O2-Si2, and H1-O1-M1 change more noticeably, with ranges of 117.6–132.3°, 117.8–130.9°, and 108.4–125.7°, respectively. The O1-M1-O2 bond angle varies slightly from 91.6° to 95.3°. Compared with Al-HY zeolite, the local structure of zeolites modified by other metal ions (Ti^{3+}, Mn^{3+}, Co^{3+}, Cu^{2+}, and Zn^{2+}) is slightly distorted, but the pore structure of the zeolite is not severely damaged, indicating that these metal ions can enter the zeolite framework.

Table 1. Optimized geometrical parameters (distances in Å, angles in °) of the different metal ions modified M-HY zeolites.

Bond and angle	Al-HY	Ti-HY	Mn-HY	Co-HY	Cu-HY	Zn-HY
O1-H1	0.971	0.976	0.972	0.970	0.967	0.968
Si1-O1	1.678	1.684	1.671	1.670	1.649	1.654
M1-O1	1.919	2.007	1.908	1.998	2.083	2.004
M1-O2	1.726	1.853	1.786	1.758	1.756	1.797
Si2-O2	1.644	1.653	1.665	1.678	1.664	1.649
Si1-O1-M1	132.3	117.6	127.2	119.3	130.6	129.8
O1-M1-O2	94.8	91.9	94.3	94.1	91.6	95.3
M1-O2-Si2	128.3	128.9	128.2	130.9	117.8	122.2
H1-O1-M1	108.4	124.8	113.0	125.7	109.3	112.4

It is of particular interest to examine how variations in the structural parameters of metal-ion-modified zeolites influence their active sites. Fig. 3 presents the calculated O-H stretching frequencies of bridging hydroxyl groups (Si-O(H)-M) located in the supercages of Y-type zeolites. The corrected O-H stretching frequency of Si-O(H)-Al is 3646 cm^{-1}, which is in excellent agreement with the experimental value (3640 cm^{-1} for the supercage [51]), confirming the reliability of the computational method employed. The other bridging hydroxyl stretching frequencies are 3499 cm^{-1} for Si-O(H)-Ti, 3607 cm^{-1} for Si-O(H)-Mn, 3653 cm^{-1} for Si-O(H)-Co, 3692 cm^{-1} for Si-O(H)-Cu and Si-O(H)-Zn. These values indicate that the O-H bond strength increases in the order: Si-O(H)-Ti < Si-O(H)-Mn < Si-O(H)-Al < Si-O(H)-Co < Si-O(H)-Zn ≈ Si-O(H)-Cu, which is consistent with the corresponding O-H bond length variations. Consequently, the Brønsted acidity follows the opposite order: Ti-HY > Mn-HY > Al-HY > Co-HY > Zn-HY ≈ Cu-HY, meaning that a lower O-H stretching frequency corresponds to a weaker O-H bond and thus stronger acidity.

Table 2 lists the Mulliken atomic charges of the main atoms in the M-HY zeolites modified with different metal ions. The electropositivity of the hydrogen atoms decreases in the order: Si-O(H)-Al > Si-O(H)-Mn > Si-O(H)-Co > Si-O(H)-Zn > Si-O(H)-Cu > Si-O(H)-Ti, indicating that different metal ions exert a certain influence on the acid strength of the zeolite. In addition, metal ion modification alters the atomic charge distribution within the zeolite framework. The electropositivity of the bridging hydroxyl groups (Si-O(H)-M) follows the order: Si-O(H)-Mn > Si-O(H)-Ti > Si-O(H)-Al > Si-O(H)-Co > Si-O(H)-Zn > Si-O(H)-Cu.

3.2 Adsorption of the Thiophene on M-HY Zeolites

Based on these findings regarding the framework and acidity of M-HY zeolites, we accordingly investigated the adsorption behavior of thiophene on these materials. When a thiophene molecule approaches the zeolite channel, the proton of the Brønsted acid site in the zeolite can interact with the double bond of the thiophene molecule, leading to the formation of a π-complex. This interaction has been directly observed by infrared spectroscopy and characterized theoretically [46,52,53,54]. Fig. 4 presents the optimized structures of the π-complexes T-M-HY (M = Al^{3+}, Ti^{3+}, Mn^{3+}, Co^{3+}, Cu^{2+}, and Zn^{2+}), and the corresponding geometric parameters are summarized in Table 3. As shown in Fig. 4, for the π-complexes (T-M-HY), the distances of C1-H1 and C2-H1 (approximately 2.2 Å and 2.3 Å, respectively) are shorter than those of C3–H1 and C4–H1 (approximately 3.2 Å and 3.6 Å, respectively). Thus, between the two double bonds of the thiophene molecule (i.e., the C1=C2 and C3=C4 bonds), the C1=C2 double bond preferentially interacts with the acidic H1 proton. As a result of the weakening of the π bond in thiophene and the O1-H1 bond in the zeolite, the C1=C2 double bond exhibits a slight elongation. The H1-O1-M1 bond angles vary by 0.3° to 3.2°, as the proton of the active site reorients toward the double bond of thiophene. The geometric parameters of the T-M-HY π-complexes are very close to those of isolated thiophene and the pristine M-HY zeolites, indicating that this weak interaction does not significantly perturb their respective structures. Specifically, the C1-H1 and C2-H1 distances are 2.140 Å and 2.237 Å for T-Al-HY, 2.179 Å and 2.357 Å for T-Ti-HY, 2.134 Å and 2.261 Å for T-Mn-HY, 2.211 Å and 2.337 Å for T-Co-HY, 2.268 Å and 2.343 Å for T-Cu-HY, and 2.209 Å and 2.291 Å for T-Zn-HY, respectively. In all complexes, the C1-H1 distances (2.134–2.268 Å) are shorter than the C2–H1 distances (2.237–2.357 Å), suggesting that the asymmetric interaction facilitates easier protonation of the C1 atom. The distance between thiophene and the acid site follows the order: T-Cu-HY > T-Co-HY > T-Ti-HY > T-Zn-HY > T-Mn-HY ≈ T-Al-HY. Among these, the T-Cu-HY complex exhibits the largest separation between thiophene and the acid site, indicating the weakest π-adsorption. In contrast, the T-Al-HY and T-Mn-HY complexes demonstrate the strongest π-adsorption, implying that thiophene molecules are more readily adsorbed on Al^{3+}- and Mn^{3+}-modified HY zeolites.

3.3 Adsorption of the Benzene on M-HY Zeolites

Similar to thiophene, benzene also interacts with Brønsted acid sites via its delocalized π-electrons. Accordingly, to enable a direct comparison with the adsorption behavior of thiophene and to elucidate the competitive mechanism between the two adsorbates, the adsorption of benzene

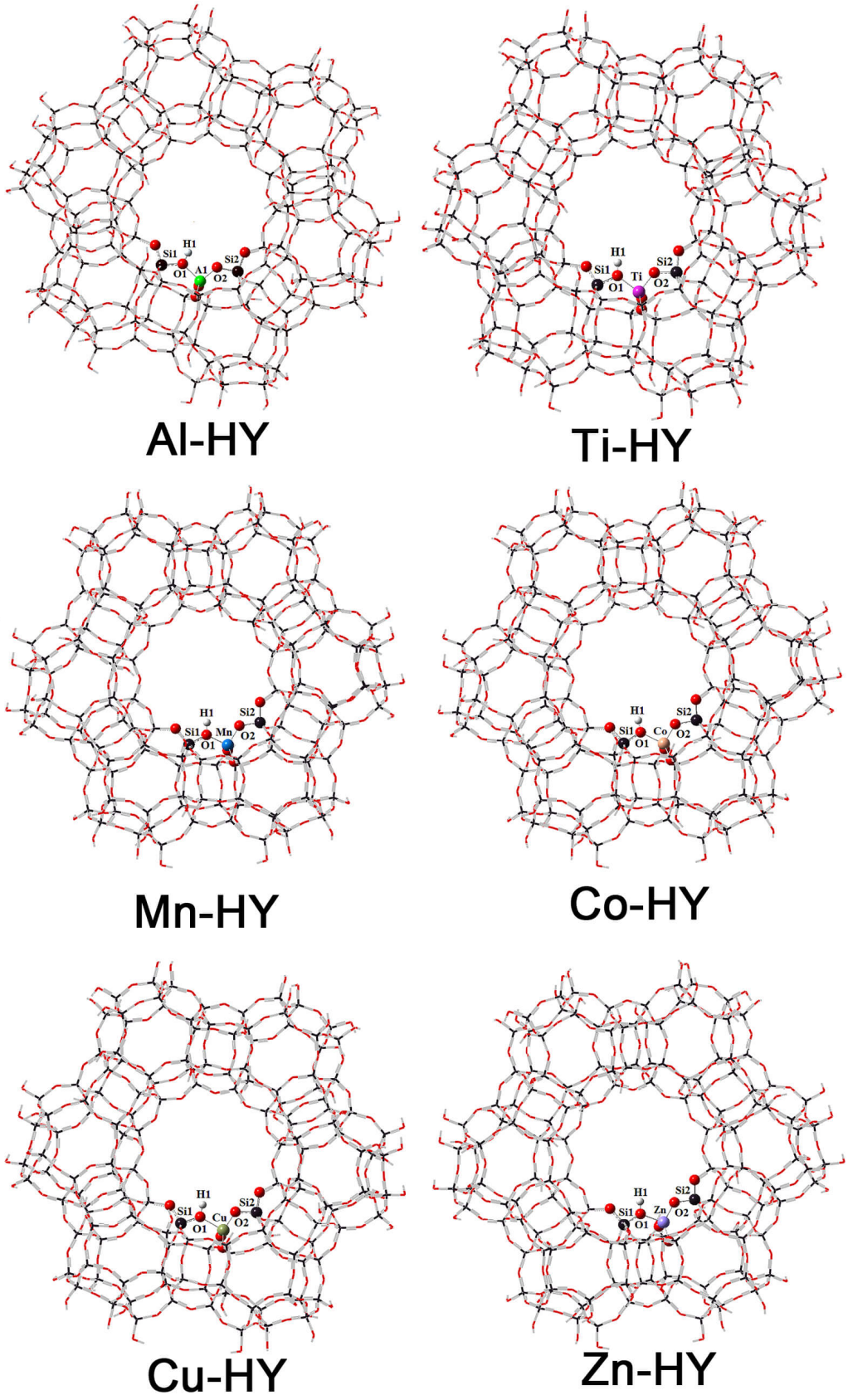

Fig. 2. Optimized structures of the different metal ions modified M-HY zeolites.

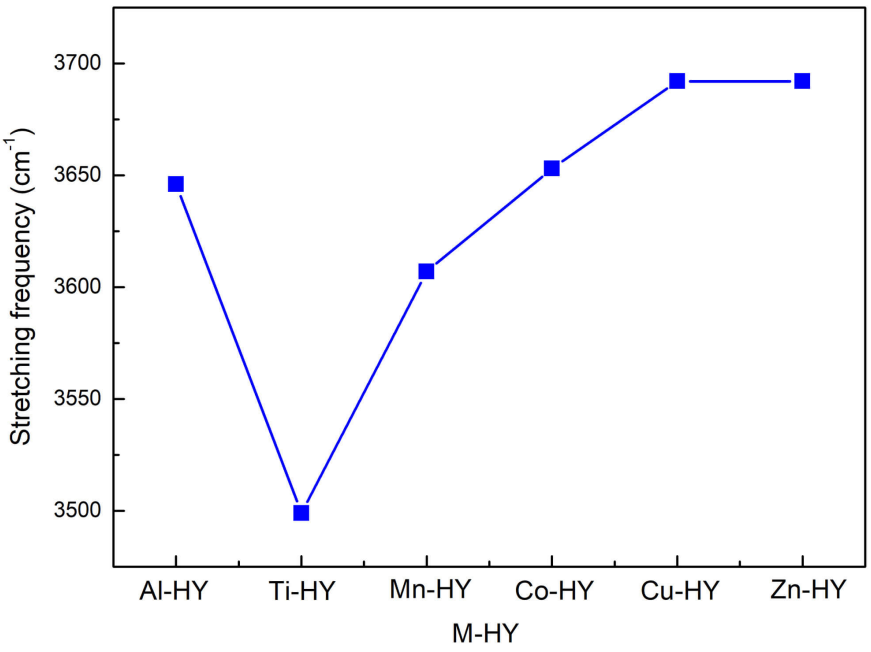

Fig. 3. O-H stretching frequencies (cm^{-1}) for M-HY zeolites.

Table 2. Mulliken main atomic charges (e) of the different metal ions modified M-HY zeolites.

Atom	Al-HY	Ti-HY	Mn-HY	Co-HY	Cu-HY	Zn-HY
H1	0.403	0.351	0.397	0.388	0.369	0.382
O1	–0.613	–0.641	–0.666	–0.676	–0.637	–0.647
Si1	0.944	0.898	0.956	0.946	0.935	0.943
M1	0.855	1.018	1.002	0.894	0.804	0.846
∑	1.589	1.626	1.689	1.552	1.471	1.524

on M-HY zeolites was also examined. The optimized structures of the π-complexes B-M-HY (M = Al^{3+}, Ti^{3+}, Mn^{3+}, Co^{3+}, Cu^{2+}, and Zn^{2+}) are illustrated in Fig. 5, and the corresponding geometric parameters are summarized in Table 4. As a benzene molecule approaches the zeolite channel, the double bond also facilitates a weak covalent interaction between the zeolite acid site and the π-electron density of the benzene molecule, resulting in the formation of a π-complex. The geometric parameters of these π-complexes are comparable to those of the corresponding isolated systems, indicating that this weak interaction does not significantly perturb the structures of either the benzene molecules or the M-HY zeolites. The primary observed difference is that both the C1=C2 double bond and the O1-H1 bond undergo slight elongation, resulting from the weakening of the π bond in the benzene molecule and the O1-H1 bond in the zeolite, respectively. The C1-H1 and C2-H1 distances are as follows: 2.205 Å and 2.344 Å for B-Al-HY, 2.273 Å and 2.535 Å for B-Ti-HY, 2.201 Å and 2.384 Å for B-Mn-HY, 2.227 Å and 2.290 Å for B-Co-HY, 2.357 Å and 2.472 Å for B-Cu-HY, and 2.284 Å and 2.386 Å for B-Zn-HY, respectively. Analogous to the adsorption behavior of thiophene molecules, the C1–H1 distance is shorter than the C2–H1 distance in all complexes, indicating that the asymmetric interaction leads to preferential protonation of the C1 atom. The distance between benzene and the acid site follows the order: B-Cu-HY > B-Ti-HY > B-Zn-HY > B-Mn-HY > B-Al-HY > B-Co-HY. Among these, the B-Cu-HY complex exhibits the largest separation between benzene and the acid site, indicating the weakest π-adsorption. Conversely, the B-Co-HY complex displays the strongest π-adsorption, suggesting that benzene molecules are most readily adsorbed on Co^{3+}-modified HY zeolites. Comparing the parameters of the B-M-HY and T-M-HY complexes, it is evident that the distances between benzene molecules and the acidic protons are greater than those between thiophene molecules and the acidic protons. This difference is likely attributable to the structural dissimilarities between benzene and thiophene.

3.4 Adsorption Energy Analysis

Although the geometric parameters of the π-complexes provide insights into adsorption preferences, a more quantitative comparison can be achieved through adsorption energy analysis. Table 5 lists the adsorption energies of thiophene and benzene on M-HY zeolites.

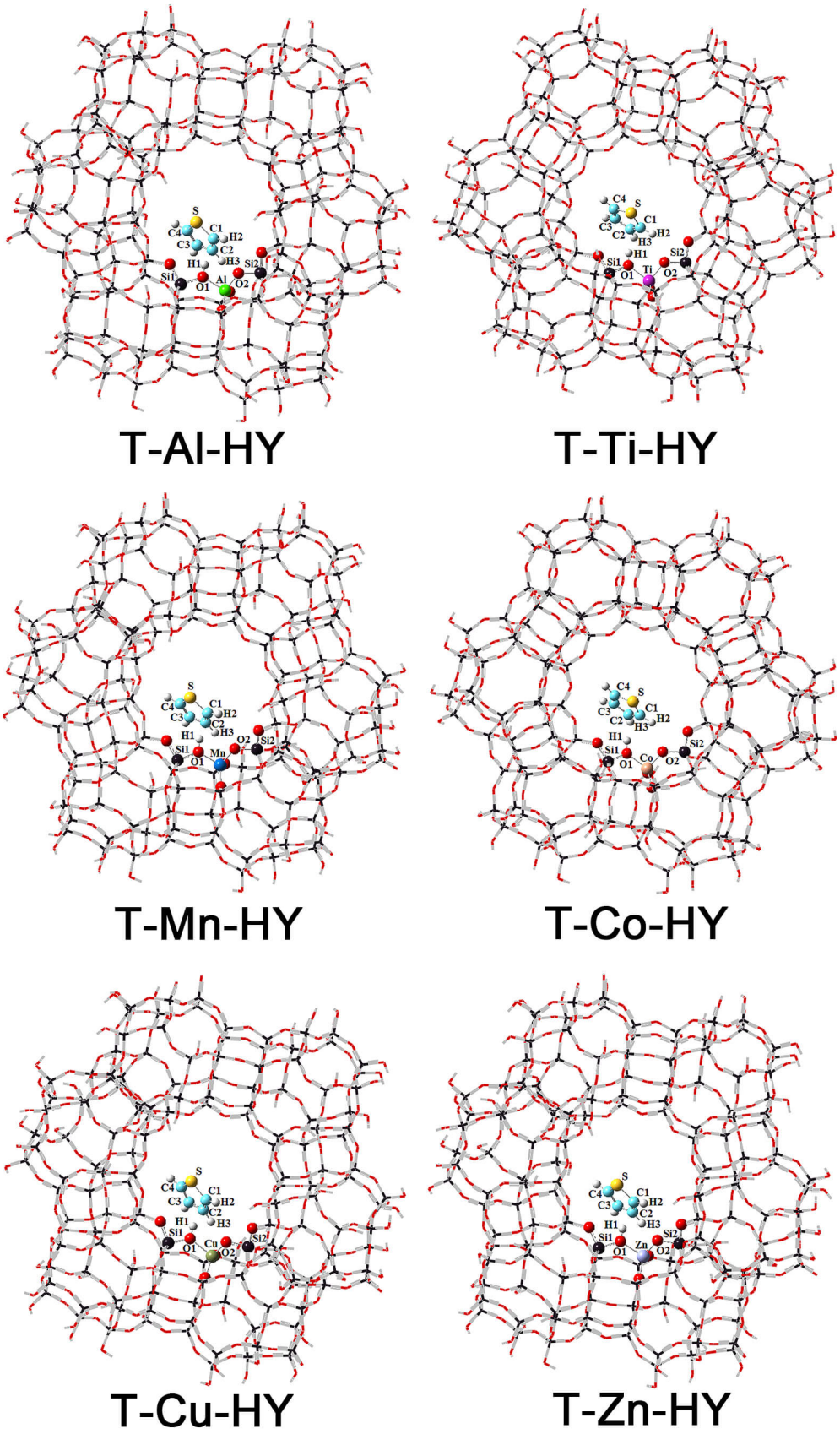

Fig. 4. Optimized structures of the π-complexes of the thiophene molecules on M-HY zeolites.

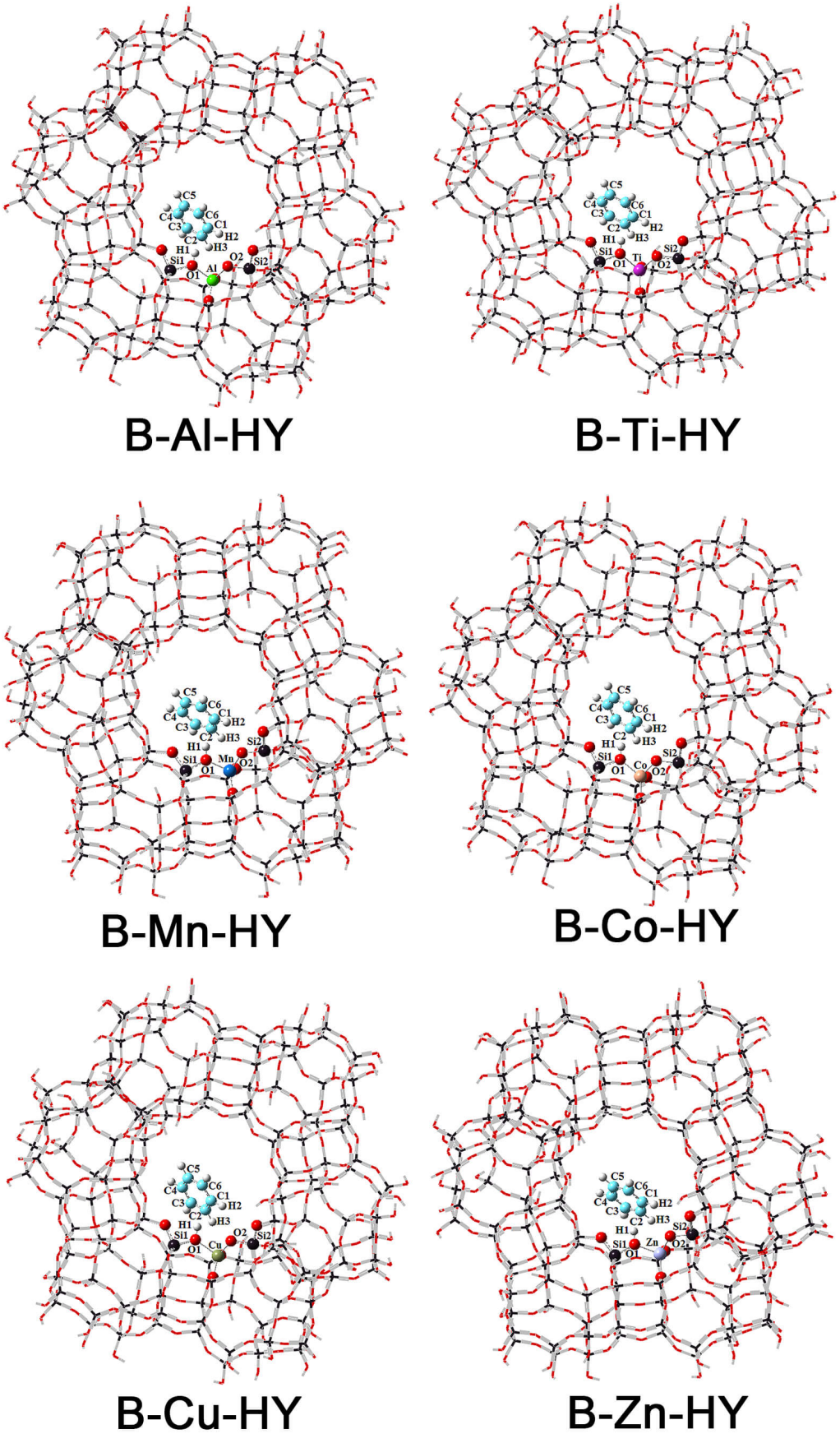

Fig. 5. Optimized structures of the π-complexes of the benzene molecules on M-HY zeolites.

Table 3. Optimized geometrical parameters (distances in Å, angles in °) of the π-complexes T-M-HY.

Bond and angle	Thiophene	T-Al-HY	T-Ti-HY	T-Mn-HY	T-Co-HY	T-Cu-HY	T-Zn-HY
C1-C2	1.367	1.375	1.374	1.375	1.374	1.373	1.374
C2-C3	1.430	1.430	1.430	1.430	1.431	1.430	1.430
C3-C4	1.367	1.368	1.367	1.368	1.367	1.368	1.368
C4-S1	1.735	1.733	1.735	1.733	1.735	1.733	1.733
S1-C1	1.735	1.739	1.739	1.739	1.738	1.737	1.738
C1-H2	1.081	1.084	1.086	1.083	1.085	1.083	1.083
C2-H3	1.084	1.086	1.085	1.086	1.085	1.085	1.086
C1-C2-C3	112.7	112.6	113.1	112.6	113.0	112.6	112.6
S1-C1-C2	111.5	111.3	110.9	111.3	111.0	111.4	111.4
C4-S1-C1	91.5	91.5	91.8	91.5	91.7	91.5	91.5
C1-H1		2.140	2.179	2.134	2.211	2.268	2.209
C2-H1		2.237	2.357	2.261	2.337	2.343	2.291
C3-H1		3.112	3.202	3.110	3.197	3.209	3.134
C4-H1		3.576	3.596	3.544	3.629	3.681	3.591
S1-H1		3.235	3.194	3.191	3.259	3.349	3.266
O1-H1		0.991	0.988	0.989	0.983	0.977	0.981
Si1-O1		1.672	1.672	1.662	1.668	1.644	1.648
M1-O1		1.904	2.003	1.903	1.966	2.078	1.986
M1-O2		1.725	1.869	1.781	1.772	1.753	1.803
Si2-O2		1.638	1.649	1.658	1.678	1.664	1.648
Si1-O1-M1		131.7	119.3	115.6	119.2	130.1	128.9
O1-M1-O2		96.5	92.3	96.0	94.7	93.6	96.2
M1-O2-Si2		129.7	127.9	129.3	131.1	120.1	123.8
H1-O1-M1		109.2	123.2	112.7	124.7	112.5	111.3

Table 4. Optimized geometrical parameters (distances in Å, angles in °) of the π complexes B-M-HY.

Bond and angle	Benzene	B-Al-HY	B-Ti-HY	B-Mn-HY	B-Co-HY	B-Cu-HY	B-Zn-HY
C1-C2	1.396	1.402	1.402	1.402	1.402	1.400	1.401
C2-C3	1.396	1.399	1.397	1.399	1.399	1.398	1.399
C3-C4	1.396	1.395	1.397	1.396	1.396	1.396	1.395
C4-C5	1.396	1.398	1.397	1.397	1.398	1.397	1.397
C5-C6	1.396	1.395	1.396	1.395	1.395	1.395	1.395
C6-C1	1.396	1.400	1.400	1.400	1.400	1.399	1.400
C1-H2	1.086	1.088	1.088	1.088	1.087	1.087	1.087
C2-H3	1.086	1.086	1.086	1.086	1.087	1.086	1.086
C1-C2-C3	120.0	119.9	120.0	119.9	119.9	119.9	119.9
C2-C3-C4	120.0	120.1	120.0	120.1	120.1	120.0	120.1
C6-C1-C2	120.0	119.8	119.8	119.8	119.8	119.9	119.9
C1-H1		2.205	2.273	2.201	2.227	2.357	2.284
C2-H1		2.344	2.535	2.384	2.290	2.472	2.386
C3-H1		3.193	3.358	3.201	3.110	3.325	3.183
C6-H1		2.997	2.967	2.936	3.015	3.159	3.038
O1-H1		0.985	0.982	0.984	0.981	0.973	0.977
Si1-O1		1.674	1.674	1.664	1.670	1.645	1.650
M1-O1		1.906	2.003	1.904	1.962	2.070	1.987
M1-O2		1.725	1.855	1.783	1.764	1.755	1.802
Si2-O2		1.638	1.649	1.658	1.677	1.660	1.647
Si1-O1-M1		131.7	118.6	127.1	119.6	129.9	128.9
O1-M1-O2		96.3	93.0	95.8	95.2	92.7	96.2
M1-O2-Si2		129.6	128.9	129.4	130.6	119.2	123.8
H1-O1-M1		110.0	123.6	114.0	124.6	115.0	112.8

Table 5. Adsorption energies of thiophene and benzene on M-HY zeolites (kJ/mol).

T-M-HY	E_{ads}	B-M-HY	E_{ads}
T-Al-HY	–78.81	B-Al-HY	–78.32
T-Ti-HY	–70.04	B-Ti-HY	–72.14
T-Mn-HY	–77.39	B-Mn-HY	–77.56
T-Co-HY	–68.91	B-Co-HY	–108.57
T-Cu-HY	–30.12	B-Cu-HY	–66.86
T-Zn-HY	–72.90	B-Zn-HY	–73.36

All adsorption energies are negative, indicating that the adsorption process is exothermic. In general, a larger absolute value of the adsorption energy (i.e., a more negative value) implies a stronger interaction between the adsorbent and the adsorbate molecules. For clarity, the following comparison of adsorption energies is based on their absolute values. The adsorption energies of thiophene on T-Al-HY and T-Mn-HY are comparable (78.81 kJ/mol and 77.39 kJ/mol, respectively) and are slightly higher than those on T-Ti-HY, T-Co-HY, and T-Zn-HY (70.04 kJ/mol, 68.91 kJ/mol, and 72.90 kJ/mol, respectively). Among all complexes, T-Cu-HY exhibits the lowest adsorption energy for thiophene, at only 30.12 kJ/mol. The order of adsorption energies for thiophene on M-HY zeolites is T-Al-HY ≈ T-Mn-HY > T-Zn-HY > T-Ti-HY ≈ T-Co-HY > T-Cu-HY, which is in agreement with the calculated geometric parameters. However, this order differs slightly from the trends inferred from the bridging OH stretching frequencies and the electronegativity of the H atom, suggesting that adsorption is influenced not only by acidity but also by the framework structure of the molecular sieve. This discrepancy arises because the introduction of different metal ions into the molecular sieve framework exerts distinct effects on both the framework geometry and the acidity. Furthermore, it is found that Al^{3+}- and Mn^{3+}-modified HY zeolites exhibit the strongest adsorption capacity for thiophene, whereas Cu^{2+}-modified HY zeolites show the weakest.

The adsorption energies of benzene on B-Al-HY and B-Mn-HY are similar (78.32 kJ/mol and 77.56 kJ/mol, respectively) and are slightly higher than those on B-Zn-HY and B-Ti-HY (73.36 kJ/mol and 72.14 kJ/mol, respectively). Among all complexes, B-Cu-HY exhibits the lowest adsorption energy for benzene at 66.86 kJ/mol, while B-Co-HY shows the highest at 108.57 kJ/mol. The order of adsorption energies of benzene on M-HY zeolites decreases as follows: B-Co-HY > B-Al-HY ≈ B-Mn-HY > B-Zn-HY ≈ B-Ti-HY > B-Cu-HY, which is consistent with the calculated geometric parameters. Similar to the case of thiophene adsorption, this order deviates from the trends inferred from the bridging OH stretching frequencies and the electronegativity of the H atom. Consequently, it is evident that Co^{3+}-modified HY zeolites possess the strongest adsorption capacity for benzene, whereas Cu^{2+}-modified HY zeolites exhibit the weakest.

Comparison of the B-M-HY and T-M-HY complexes reveals certain numerical differences in the adsorption energies of thiophene and benzene on M-HY zeolites. Specifically, the adsorption energies of thiophene and benzene on HY zeolites modified with Al^{3+}, Ti^{3+}, Mn^{3+}, and Zn^{2+} are comparable, all falling within the range of 70–79 kJ/mol, indicating poor adsorption selectivity between thiophene and benzene when both coexist in the system. In contrast, the adsorption behaviors of thiophene and benzene on Co^{3+}- and Cu^{2+}-modified HY zeolites exhibit pronounced differences. The adsorption energies of benzene on Co-HY and Cu-HY zeolites are substantially higher than those of thiophene, exceeding them by 39.66 kJ/mol and 36.74 kJ/mol, respectively. This suggests that Co^{3+}- and Cu^{2+}-modified HY zeolites possess higher adsorption selectivity for benzene, while being unfavorable for thiophene removal. Consequently, the preferential adsorption of benzene leads to a decrease in both the desulfurization activity and selectivity of the molecular sieve.

Experimental studies by Takahashi et al. [55] reported that the adsorption heats of thiophene and benzene on low-silica Y-type zeolites are 79.91–93.72 kJ/mol and 71.12–91.21 kJ/mol, respectively, while on high-silica Y-type zeolites, they are 33.05–46.86 kJ/mol and 27.61–54.81 kJ/mol, respectively. Comparing these experimental data, the theoretical adsorption energies of thiophene and benzene on Y-type zeolites modified with Al^{3+}, Ti^{3+}, Mn^{3+}, Co^{3+}, and Zn^{2+} (68.91–78.81 kJ/mol and 72.14–108.57 kJ/mol, respectively) are relatively close to the experimental values obtained under low-silica conditions. In contrast, on the Cu^{2+}-modified Y-type zeolite, the theoretical adsorption energies (30.12 kJ/mol for thiophene and 66.86 kJ/mol for benzene) are closer to the experimental values measured under high-silica conditions. This finding is also consistent with the results of Monte Carlo simulations reported in Ref. [56]. Overall, although there are some numerical discrepancies between the theoretical and experimental values, their variation trends are generally consistent, indicating that the adopted metal-modified Y-type zeolite model can adequately describe the main adsorption characteristics of thiophene and benzene on this class of materials.

4. Discussion

The above results indicate that the adsorption behavior of thiophene and benzene on M-HY zeolites is collectively determined by the zeolite's acid sites, microporous structure, and the intrinsic structural characteristics of the adsorbate molecules. The introduction of different metal ions into the zeolite framework simultaneously modulates the local geometry and the Brønsted acidity of the bridging hydroxyl groups (Si-O(H)-M). Minor local structural distortions occur in the vicinity of acid sites within the metal-modified zeolites. The calculated O-H stretching frequen-

cies reveal that the acidity strength follows the order: Ti-HY > Mn-HY > Al-HY > Co-HY > Zn-HY ≈ Cu-HY. Notably, the adsorption energies do not strictly adhere to this acidity sequence. For instance, although Ti^{3+}-modified HY exhibits relatively strong acidity, it shows only moderate adsorption energies for thiophene (70.04 kJ/mol) and benzene (72.14 kJ/mol). In contrast, Co^{3+}-modified HY, despite possessing moderate acidity, demonstrates the highest adsorption energy for benzene (108.57 kJ/mol) and a relatively lower adsorption energy for thiophene (68.91 kJ/mol). This discrepancy suggests that the adsorption process is governed by three synergistic factors: (i) covalent or hydrogen-bonding interactions between the adsorbate and Brønsted acid sites [57,58]; (ii) van der Waals interactions arising from the microporous structure of the zeolite [59]; and (iii) the intrinsic structural characteristics of the adsorbate molecules. The adsorption of unsaturated organic compounds on zeolites is thus controlled by the cooperative effect of these three factors.

The interaction between thiophene/benzene and the active sites of zeolites follows a π-complexation mechanism, with calculated adsorption energies ranging from 30.12 to 108.57 kJ/mol. The relatively weak strength of this interaction enables the removal of adsorbed molecules by heating or solvent washing, thereby endowing the adsorbent with good regeneration performance and the potential for multiple adsorption–desorption cycles. The theoretically calculated adsorption energies are in reasonable agreement with the experimentally measured adsorption heats (27.61–93.72 kJ/mol) [55], indicating that the 144T cluster model employed can adequately capture the major adsorption characteristics of thiophene and benzene on metal-modified Y-type zeolites, thereby validating the reliability of the ONIOM computational strategy. However, a certain discrepancy between the two remains, which may be attributed to the following factors: on the one hand, the experimentally measured adsorption heats reflect the properties of real zeolite surfaces (including multiple acid sites, structural defects, and adsorbate–adsorbate interactions) as well as the inherent limitations of the measurement methods themselves [60]; on the other hand, the theoretically calculated adsorption energies correspond to the intrinsic adsorption internal energies of an idealized model under zero-coverage conditions.

From the perspective of adsorption selectivity, Al^{3+}-, Ti^{3+}-, Mn^{3+}-, and Zn^{2+}-modified HY exhibit similar adsorption energies for thiophene and benzene (70–79 kJ/mol), suggesting negligible discrimination between the two species when they coexist in the system. According to the π-adsorption mechanism, an increase in the number of zeolite acid sites simultaneously enhances the adsorption capacity for both thiophene and benzene [61]. Therefore, relying solely on increasing acid sites is unlikely to achieve high selectivity. In contrast, Co^{3+}- and Cu^{2+}-modified HY exhibit pronounced differences in adsorption energy toward the two adsorbates, with benzene adsorption energies being 39.66 and 36.74 kJ/mol higher than those of thiophene, respectively. This indicates that Co^{3+} and Cu^{2+} modification unexpectedly favors benzene adsorption, rendering these materials unsuitable for selective thiophene removal. It is worth noting that none of the investigated metal ions show a preferential adsorption for thiophene, a finding that highlights selectivity as a core challenge in the design of desulfurization adsorbents.

Limitation

Although this computational study provides valuable insights, several limitations should be acknowledged. First, the ONIOM(B3LYP/UFF) method achieves a balance between accuracy and computational cost, but it is inherently approximate. The B3LYP functional may not fully capture dispersion interactions, although the UFF force field partially compensates for this. More accurate methods, such as DFT-D3, could provide more precise results but at a significantly higher computational cost. Second, although the 144T cluster model contains a complete supercage, it remains a finite truncation of an infinite framework. Sites in the sodalite cage and double six-membered ring (D6R) are not included in the model, and the absence of edge effects and long-range periodicity may introduce minor inaccuracies, particularly in describing long-range electrostatic interactions and confinement effects. Third, the present study does not consider co-adsorption effects; no explicit co-adsorption model with thiophene and benzene molecules simultaneously present in the same supercage was constructed, whereas real fuel systems contain multiple competing species (e.g., other aromatics, water, sulfur-containing compounds). Fourth, this study only considers the adsorption mechanism involving π-complexation through Brønsted acid sites. The potential direct S-M coordination between thiophene sulfur and metal cations, which has been proposed in previous studies [32,33], has not been systematically investigated.

Despite these limitations, the present study provides a thermodynamic perspective on adsorption selectivity, while explicit co-adsorption mechanisms require further investigation. Future work should aim to address these limitations to further elucidate the nature of adsorption selectivity.

5. Conclusions

In this study, the adsorption selectivity mechanism of thiophene and benzene over a series of metal-modified M-HY zeolites (M = Al^{3+}, Ti^{3+}, Mn^{3+}, Co^{3+}, Cu^{2+}, Zn^{2+}) was theoretically investigated using the ONIOM(B3LYP/UFF) method. The computational results indicate that all six metal ions can be incorporated into the framework of the Y-type zeolite. Although this incorporation causes slight local structural distortions, it does not destroy the main pore structure of the zeolite. The introduction of metal ions significantly modulates the strength of Brønsted acid sites and

the charge distribution of the framework atoms. The order of acid strength for the various zeolites is: Ti-HY > Mn-HY > Al-HY > Co-HY > Zn-HY ≈ Cu-HY, indicating that Ti-HY possesses the strongest acidity, while Cu-HY and Zn-HY exhibit the weakest acidity. Both thiophene and benzene form π-complexes with the Brønsted acid sites of the zeolite through π-coordination. This type of interaction falls within the realm of weak interactions and does not significantly alter the intrinsic structures of the adsorbate or the adsorbent.

The theoretical adsorption energies of thiophene and benzene on M-HY zeolites are 30.12–78.81 kJ/mol and 66.86–108.57 kJ/mol, respectively. Al^{3+}- and Mn^{3+}-modified HY zeolites exhibit the strongest adsorption for thiophene (78.81 and 77.39 kJ/mol, respectively), while Co^{3+}-modified HY shows the strongest adsorption for benzene (108.57 kJ/mol). In contrast, Cu^{2+}-modified HY displays the weakest adsorption for both adsorbates (30.12 and 66.86 kJ/mol, respectively). The variation in adsorption energies does not fully align with the order of acid strength, indicating that the adsorption performance is collectively influenced by acid strength, framework structure, and adsorbate molecular structure, rather than being determined by a single factor.

The adsorption energies of thiophene and benzene on Al^{3+}-, Ti^{3+}-, Mn^{3+}-, and Zn^{2+}-modified HY zeolites are similar (70–79 kJ/mol). When the two adsorbates coexist, the preferential adsorption of benzene occurs, which is detrimental to the desulfurization selectivity in practical fuel oil systems. Cu^{2+}- and Co^{3+}-modified HY exhibit significantly better adsorption for benzene (66.86 and 108.57 kJ/mol, respectively) than for thiophene (30.12 and 68.91 kJ/mol, respectively). None of the investigated metal ions show an inherent adsorption preference for thiophene. Although metal ion modification is an effective approach to tune the adsorption performance of zeolites, simply enhancing acidity or π-complexation is insufficient to achieve highly selective desulfurization; instead, specific interactions between the adsorbent and sulfur atoms (e.g., S-M coordination bonds) must be strengthened. Future efforts should focus on strategies to enhance thiophene selectivity, such as pore size tailoring, hydrophobic modification, or the design of multifunctional adsorbents that combine selective sulfur adsorption with aromatic repulsion.

In summary, this study reveals the adsorption selectivity mechanism of thiophene and benzene on metal-modified Y-type zeolites at the atomic level. Although none of the investigated materials achieve preferential adsorption of thiophene, this work identifies the key factors governing adsorption selectivity, thereby providing important theoretical guidance for the rational design of next-generation adsorbents for deep desulfurization of fuel oils.

Availability of Data and Materials

The datasets used or analyzed during the current study are available from the corresponding author on reasonable request.

Author Contributions

YHG, MHX and GXP designed the research. YHG, QZ and KYW performed the theoretical calculations. MHX and QZ carried out the data processing. YHG drafted the manuscript. GXP and KYW reviewed and edited the manuscript. All authors contributed to editorial changes in the manuscript. All authors read and approved the final manuscript. All authors have participated sufficiently in the work and agreed to be accountable for all aspects of the work.

Ethics Approval and Consent to Participate

Not applicable.

Acknowledgment

We are grateful to the C3S2 computing center in Huzhou Normal University for calculation support.

Funding

This research was funded by Zhejiang Provincial Natural Science Foundation of China (LY14B060006), the "Pioneer" and "Leading Goose" R&D Program of Zhejiang (2023C01112) and the Public Welfare Application Research Project of Huzhou City (2021GZ09).

Conflicts of Interest

The authors declare no conflicts of interest. The author GXP is employed by Zhejiang Huayuan Pigment Co., Ltd. However, Zhejiang Huayuan Pigment Co., Ltd., had no involvement in the actual planning, or interpretation of the article.

References

[1] Wu P, Ma S, Zhu W. Green pathways to low-sulfur diesel: advances and challenges in desulfurization technologies. Green Chemistry. 2026; 28: 37–95. https://doi.org/10.1039/D5GC04160K

[2] Khalid A, Khalid AR, Farhan A, Arooj Y, Zahid M, Qamar MA, et al. Emerging desulfurization technologies and cutting-edge solvents for sulfur compounds removal from liquid fuels – a comprehensive review. Separation and Purification Technology. 2025; 379: 134782. https://doi.org/10.1016/j.seppur.2025.134782

[3] Gooneh-Farahani S, Anbia M. A review of advanced methods for ultra-deep desulfurization under mild conditions and the absence of hydrogen. Journal of Environmental Chemical Engineering. 2023; 11: 108997. https://doi.org/10.1016/j.jece.2022.108997

[4] Garba ZN, Zango ZU, Adamu H, Haruna A, Menkiti ND, Danmallam UN, et al. A review on zeolites for adsorptive desulfurization of crude oil and natural gas: Kinetics, isotherms,

and thermodynamics studies. Progress in Engineering Science. 2025; 2: 100063. https://doi.org/10.1016/j.pes.2025.100063
[5] Khan NA, Kim CM, Jhung SH. Adsorptive desulfurization using Cu–Ce/metal–organic framework: Improved performance based on synergy between Cu and Ce. Chemical Engineering Journal. 2017; 311: 20–27. https://doi.org/10.1016/j.cej.2016.11.067
[6] Chen Z, Ling L, Wang B, Fan H, Shangguan J, Mi J. Adsorptive desulfurization with metal-organic frameworks: A density functional theory investigation. Applied Surface Science. 2016; 387: 483–490. https://doi.org/10.1016/j.apsusc.2016.06.078
[7] Naseri S, Moradi G, Ghanadi T. Preparation of activated carbon from waste tea and its performance in adsorptive desulfurization of model fuel. International Journal of Chemical Reactor Engineering. 2025; 23: 223–231. https://doi.org/10.1515/ijcre-2024-0232
[8] Fu RX, Zha YP, Huang CF, Wang QQ, Xiong ZJ, Liu MM, et al. Metal-organic frameworks in adsorption desulfurization: Recent progress, new trends and future perspectives. Coordination Chemistry Reviews. 2026; 548: 217185. https://doi.org/10.1016/j.ccr.2025.217185
[9] Liu C, He Y, Hu Y, Xia Y, Wang H. Efficient adsorptive desulfurization of dibenzothiophene from waste oil using cobalt-modified zeolite for sustainable oil recovery. Chemical Engineering Science. 2026; 327: 123691. https://doi.org/10.1016/j.ces.2026.123691
[10] Ghadiri M, Ghaemi A, Shayanmehr M. A comprehensive review on exploring the potential and behavior of carbon-based adsorbents in the adsorptive desulfurization processes. Fuel. 2026; 404: 136222. https://doi.org/10.1016/j.fuel.2025.136222
[11] Ahmed I, Jhung SH. Adsorptive desulfurization and denitrogenation using metal-organic frameworks. Journal of Hazardous Materials. 2016; 301: 259–276. https://doi.org/10.1016/j.jhazmat.2015.08.045
[12] Jafarabadi H, Mansouri M, Shayanmehr M, Ghaemi A. Mechanisms, challenges, and future perspectives of adsorptive desulfurization using zeolite-based adsorbents: a review. Environmental Science and Pollution Research International. 2025; 32: 11350–11402. https://doi.org/10.1007/s11356-025-36333-3
[13] Zheng T, Fan H, Zhao J, Fu J, Ye S, Ali S, et al. Tuning electron configuration of metal sites for the diesel adsorptive desulfurization over ion-exchanged zeolite Y. Journal of Environmental Chemical Engineering. 2024; 12: 113751. https://doi.org/10.1016/j.jece.2024.113751
[14] Yu M, Zhang XF, Yang S, Yao J. NaY zeolite incorporated alginate beads for efficient adsorption desulfurization. Chemical Engineering Science. 2025; 306: 121237. https://doi.org/10.1016/j.ces.2025.121237
[15] Salem ABSH, Hamid HS. Removal of Sulfur Compounds from Naphtha Solutions Using Solid Adsorbents. Chemical Engineering and Technology. 1997; 20: 342–347. https://doi.org/10.1002/ceat.270200511
[16] Sarda KK, Bhandari A, Pant KK, Jain S. Deep desulfurization of diesel fuel by selective adsorption over Ni/Al2O3 and Ni/ZSM-5 extrudates. Fuel. 2012; 93: 86–91. https://doi.org/10.1016/j.fuel.2011.10.020
[17] Tian F, Yang X, Shi Y, Jia C, Chen Y. Adsorptive desulfurization over hierarchical beta zeolite by alkaline treatment. Journal of Natural Gas Chemistry. 2012; 21: 647–652. https://doi.org/10.1016/S1003-9953(11)60414-3
[18] Subhan F, Liu BS. Acidic sites and deep desulfurization performance of nickel supported mesoporous AlMCM-41 sorbents. Chemical Engineering Journal. 2011; 178: 69–77. https://doi.org/10.1016/j.cej.2011.10.013
[19] Lee KX, Valla JA. Investigation of metal-exchanged mesoporous Y zeolites for the adsorptive desulfurization of liquid fuels. Applied Catalysis B: Environmental. 2017; 201: 359–369. https://doi.org/10.1016/j.apcatb.2016.08.018
[20] Wang J, Zhao J, Wen Z, Wei X, Liao J, Chang L, et al. Regulating cerium location in Y zeolite and its influence on adsorptive desulfurization for thiophene in benzene. Separation and Purification Technology. 2025; 353: 128517. https://doi.org/10.1016/j.seppur.2024.128517
[21] Sokol HJ, Lee KX, Valla JA. The mechanism of adsorptive desulfurization on Cu and Ce exchanged Y zeolite using density functional theory. Computational Materials Science. 2024; 235: 112813. https://doi.org/10.1016/j.commatsci.2024.112813
[22] Song H, Wan X, Dai M, Zhang J, Li F, Song H. Deep desulfurization of model gasoline by selective adsorption over Cu-Ce bimetal ion-exchanged Y zeolite. Fuel Processing Technology. 2013; 116: 52–62. https://doi.org/10.1016/j.fuproc.2013.04.017
[23] Yoosuk B, Silajan A, Prasassarakich P. Deep adsorptive desulfurization over ion-exchanged zeolites: Individual and simultaneous effect of aromatic and nitrogen compounds. Journal of Cleaner Production. 2020; 248: 119291. https://doi.org/10.1016/j.jclepro.2019.119291
[24] Bulut B, Atakül H, Aksoylu AE, Tantekin-Ersolmaz ŞB. Deep adsorptive desulfurization of liquefied petroleum gas over Cu ion-exchanged Y zeolite. Separation and Purification Technology. 2024; 338: 126431. https://doi.org/10.1016/j.seppur.2024.126431
[25] Jiang B, Zhu T, Jiang N, Gong M, Yang G, Li F, et al. Ultra-deep adsorptive removal over hierarchically structured AgCeY zeolite from model gasoline with high competitor content. Journal of Cleaner Production. 2021; 297: 126582. https://doi.org/10.1016/j.jclepro.2021.126582
[26] Zhang S, Zhang Y, Huang S, Wang P, Tian H. Mechanistic investigations on the adsorption of thiophene over Zn3NiO4 bimetallic oxide cluster. Applied Surface Science. 2012; 258: 10148–10153. https://doi.org/10.1016/j.apsusc.2012.06.096
[27] Hernández-Maldonado AJ, Yang FH, Qi G, Yang RT. Desulfurization of transportation fuels by π-complexation sorbents: Cu(I)-, Ni(II)-, and Zn(II)-zeolites. Applied Catalysis B: Environmental. 2005; 56: 111–126. https://doi.org/10.1016/j.apcatb.2004.06.023
[28] Lv N, Zhu T, Luo D, Yi W, Dai C, Li H, et al. The origin of selective adsorption desulfurization by Fe single atom adsorbents on hexagonal boron nitride surface. Separation and Purification Technology. 2025; 359: 130641. https://doi.org/10.1016/j.seppur.2024.130641
[29] Han B, Chu YY, Zheng AM, Deng F. Adsorption Structure and Energy of Pyridine Confined inside Zeolite Pores. Acta Physico-Chimica Sinica. 2012; 28: 315–323. https://doi.org/10.3866/PKU.WHXB201111232 (In Chinese)
[30] Ma X, Velu S, Kim JH, Song C. Deep desulfurization of gasoline by selective adsorption over solid adsorbents and impact of analytical methods on ppm-level sulfur quantification for fuel cell applications. Applied Catalysis B: Environmental. 2005; 56: 137–147. https://doi.org/10.1016/j.apcatb.2004.08.013
[31] Wang YH, Yang RT, Heinzel JM. Desulfurization of jet fuel by π-complexation adsorption with metal halides supported on MCM-41 and SBA-15 mesoporous materials. Chemical Engineering Science. 2008; 63: 356–365. https://doi.org/10.1016/j.ces.2007.09.002
[32] Tian F, Wu W, Jiang Z, Liang C, Yang Y, Ying P, et al. The study of thiophene adsorption onto La(III)-exchanged zeolite NaY by FT-IR spectroscopy. Journal of Colloid and Interface Science. 2006; 301: 395–401. https://doi.org/10.1016/j.jcis.2006.05.017
[33] Li F, Song L, Duan L, Li X, Sun Z. A frequency response study of thiophene adsorption in zeolite catalysts. Applied Surface Science. 2007; 253: 8802–8809. https://doi.org/10.1016/j.apsusc.2007.05.010

[34] Jiang M, Ng FTT. Adsorption of benzothiophene on Y zeolites investigated by infrared spectroscopy and flow calorimetry. Catalysis Today. 2006; 116: 530–536. https://doi.org/10.1016/j.cattod.2006.06.034
[35] Wang L, Sun Z, Ding Y, Chen Y, Li Q, Xu M, et al. A theoretical study of thiophenic compounds adsorption on cation-exchanged Y zeolites. Applied Surface Science. 2011; 257: 7539–7544. https://doi.org/10.1016/j.apsusc.2011.03.115
[36] Gao X, Geng W, Zhang H, Zhao X, Yao X. Thiophenic compounds adsorption on Na(I)Y and rare earth exchanged Y zeolites: a density functional theory study. Journal of Molecular Modeling. 2013; 19: 4789–4795. https://doi.org/10.1007/s00894-013-1954-1
[37] Jansen A, Ruangpornvisuti V. An ONIOM investigation of reaction mechanisms of propylene glycol dehydration over H-ZSM-5 and H-MOR catalysts. Journal of Molecular Catalysis A: Chemical. 2012; 363: 171–177. https://doi.org/10.1016/j.molcata.2012.06.006
[38] Nie X, Janik MJ, Guo X, Liu X, Song C. Reaction mechanism of tert-butylation of phenol with tert-butyl alcohol over H-β zeolite: An ONIOM study. Catalysis today. 2011: 165: 120–128. https://doi.org/10.1016/j.cattod.2010.11.070
[39] Chu ZK, Fu G, Guo W, Xu X. Exploring the Sodium Cation Location and Aluminum Distribution in ZSM-5: A Systematic Study by the Extended ONIOM (XO) Method. The Journal of Physical Chemistry C. 2011; 115: 14754–14761. https://doi.org/10.1021/jp201454t
[40] Lu M, Gudala S, Liu Z, Sharma A, Liu X, Yang J. Catalytic benzylation of arenes using metal-ion modified HY zeolites for sustainable synthesis. Materials Chemistry and Physics. 2024; 328: 130034. https://doi.org/10.1016/j.matchemphys.2024.130034
[41] Liu S, Ren J, Zhu S, Zhang H, Lv E, Xu J, Li YW. Synthesis and characterization of the Fe-substituted ZSM-22 zeolite catalyst with high n-dodecane isomerization performance. Journal of Catalysis. 2015; 330: 485–496. https://doi.org/10.1016/j.jcat.2015.07.027
[42] Olson DH, Dempsey E. The crystal structure of the zeolite hydrogen faujasite. Journal of Catalysis. 1969; 13: 221–231. https://doi.org/10.1016/0021-9517(69)90395-9
[43] Rappe AK, Casewit CJ, Colwell KS, Goddard III WA, Skiff WM. UFF, a full periodic table force field for molecular mechanics and molecular dynamics simulations. Journal of the American chemical society. 1992; 114: 10024–10035. https://doi.org/10.1021/ja00051a040
[44] Kasuriya S, Namuangruk S, Treesukol P, Tirtowidjojo M, Limtrakul J. Adsorption of ethylene, benzene, and ethylbenzene over faujasite zeolites investigated by the ONIOM method. Journal of Catalysis. 2003; 219: 320–328. https://doi.org/10.1016/S0021-9517(03)00213-6
[45] Rungsirisakun R, Jansang B, Pantu P, Limtrakul J. The adsorption of benzene on industrially important nanostructured catalysts (H-BEA, H-ZSM-5, and H-FAU): confinement effects. Journal of molecular structure. 2005; 733: 239–246. https://doi.org/10.1016/j.molstruc.2004.09.002
[46] Namuangruk S, Tantanak D, Limtrakul J. Application of ONIOM calculations in the study of the effect of the zeolite framework on the adsorption of alkenes to ZSM-5. Journal of Molecular Catalysis A: Chemical. 2006; 256: 113–121. https://doi.org/10.1016/j.molcata.2006.04.060
[47] Scott AP, Radom L. Harmonic vibrational frequencies: An evaluation of Hartree-Fock, Møller-Plesset, quadratic configuration interaction, density functional theory, and semiempirical scale factors. The Journal of Physical Chemistry. 1996; 100: 16502–16513. https://doi.org/10.1021/jp960976r
[48] Frisch MJ, Trucks GW, Schlegel HB, Scuseria GE, Robb MA, Cheeseman JR, et al. Gaussian 03 (Revision B.04), Gaussian, Inc.: Pittsburgh, PA. 2003.
[49] Barthomeuf D. Zeolite acidity dependence on structure and chemical environment: correlations with catalysis. Materials Chemistry and Physics. 1987; 17: 49–71. https://doi.org/10.1016/0254-0584(87)90048-4
[50] Reddy KM, Moudrakovski I, Sayari A. Synthesis of mesoporous vanadium silicate molecular sieves. Journal of the Chemical Society, Chemical Communications. 1994; 30: 1059–1060. https://doi.org/10.1039/C39940001059
[51] Ward JW. The location of hydroxyl groups in hydrogen Y zeolite. The Journal of Physical Chemistry. 1967; 71: 3106. https://doi.org/10.1021/j100868a071
[52] Kondo JN, Domen K, Wakabayashi F. Double bond migration of 1-butene without protonated intermediate on D-ZSM-5. Microporous and Mesoporous Materials. 1998; 21: 429–437. https://doi.org/10.1016/S1387-1811(98)00004-3
[53] Kondo JN, Domen K. IR observation of adsorption and reactions of olefins on H-form zeolites. Journal of Molecular Catalysis A: Chemical. 2003; 199: 27-38. https://doi.org/10.1016/S1381-1169(03)00015-3
[54] Soscun H, Hernández J, Castellano O, Arrieta F, Ruette F, Sierralta A, et al. The interaction of cis-2-butene over a 10-ring Brönsted acid site of zeolite: a theoretical study. Journal of Molecular Catalysis A: Chemical. 2003; 192: 63–72. https://doi.org/10.1016/S1381-1169(02)00118-8
[55] Takahashi A, Yang FH, Yang RT. New Sorbents for Desulfurization by π-Complexation: Thiophene/Benzene Adsorption. Industrial and Engineering Chemistry Research. 2002; 41: 2487–2496. https://doi.org/10.1021/ie0109657
[56] Ju SG, Zeng YP, Xing WH, Chen CL. Computer simulation of the adsorption of thiophene in all-silica Y and Na-Y. Langmuir. 2006; 22: 8353–8358. https://doi.org/10.1021/la0601861
[57] Mortier WJ. Electronegativity equalization and solid state chemistry of zeolites. Studies in Surface Science and Catalysis. 1988; 37: 253–268. https://doi.org/10.1016/S0167-2991(09)60603-0
[58] Datka J, Boczar M. Interaction of benzene and hexane molecules with OH-groups of various acid strengths in NaHZSM-5 zeolite. Reaction Kinetics and Catalysis Letters. 1993; 51: 161–166. https://doi.org/10.1007/BF02062491
[59] Derouane EG, Andre JM, Lucas AA. Surface curvature effects in physisorption and catalysis by microporous solids and molecular sieves. Journal of Catalysis. 1988; 110: 58–73. https://doi.org/10.1016/0021-9517(88)90297-7
[60] Ng FTT, Rahman A, Ohasi T, Jiang M. A study of the adsorption of thiophenic sulfur compounds using flow calorimetry. Applied Catalysis B: Environmental. 2005; 56: 127–136. https://doi.org/10.1016/j.apcatb.2004.07.018
[61] Liao JJ, Bao WR, Chang LP. An approach to study the desulfurization mechanism and the competitive behavior from aromatics: A case study on CeY zeolite. Fuel Processing Technology. 2015; 140: 104–112. https://doi.org/10.1016/j.fuproc.2015.08.036